Research Square

Preprints are preliminary reports that have not undergone peer review.
They should not be considered conclusive, used to inform clinical practice,
or referenced by the media as validated information.

Evaluating Machine Learning and Deep Learning Models for Predicting Rice Vegetation Condition in Acadia, Louisiana

Desmond Fosuhene
University of North Carolina at Greensboro
Dorcas Twumwaa Gyan
dorcas.gyan@sus.edu

Southern University and A&M College
Kingsford Kobina Annan
Southern University and A&M College
Theodora Mary Fletcher
The University of Toledo
Bhuwan Thapa
University of North Carolina at Greensboro
Ebenezer Nana Kwaku Boateng
Independent Scholar

Research Article

Keywords: GeoAI, Rice, Vegetation, Acadia, Louisiana

Posted Date: October 5th, 2026

DOI: https://doi.org/10.21203/rs.3.rs-10989222/v1

License: This work is licensed under a Creative Commons Attribution 4.0 International License.
Read Full License

Additional Declarations: No competing interests reported.

Evaluating Machine Learning and Deep Learning Models for Predicting Rice Vegetation Condition in Acadia, Louisiana

Desmond Fosuhene[1], Dorcas Twumwaa Gyan[2*], Kingsford Kobina Annan[2], Theodora Mary Fletcher[3], Bhuwan Thapa[1], Ebenezer Nana Kwaku Boateng[4]

[1]Department of Geography, Environment and Sustainability, University of North Carolina at Greensboro, Greensboro, NC, 27412. Email: d_fosuhene@uncg.edu
[2]Southern University and A&M College, Baton Rouge, LA, 70807. Email: dorcas.gyan@sus.edu
[3]Department of Geography and Planning, The University of Toledo, Toledo, OH, USA
[4]Independent Scholar, Tempe, AZ. Email: enkboateng4@gmail.com
*Corresponding author's email: dorcas.gyan@sus.edu

Abstract

Purpose: Rice production is increasingly affected by climate variability, and many rice-growing regions lack the ground-observation infrastructure needed for timely crop-condition assessment. This study evaluated seven machine learning and deep learning models for predicting rice vegetation condition using satellite-derived spectral indices and environmental variables, with the aim of identifying robust modelling approaches and key predictors for scalable, satellite-based agricultural monitoring.

Methods: Landsat-derived spectral indices (NDVI, NDWI, NDMI) were integrated with climate and terrain variables across 12,544 rice field-seasons in Acadia Parish, Louisiana, from 2008 to 2025. Year fixed effects were applied to control for inter-annual confounds, and seven models; linear regression, ridge regression, random forest, gradient boosting, XGBoost, LightGBM, and a deep neural network, were evaluated using five-fold random cross-validation. Variable contributions were assessed using impurity-based and permutation feature importance.

Results: All seven models achieved high predictive accuracy, with Gradient Boosting yielding the highest coefficient of determination (R^2 = 0.960 ± 0.002). Permutation feature importance analysis showed that the Normalized Difference Water Index (NDWI) was the dominant predictor (ΔR^2 = 1.708), far exceeding the Normalized Difference Moisture Index (NDMI; ΔR^2 = 0.034) and all other environmental variables ($\Delta R^2 \leq 0.002$).

Conclusion: In flood-irrigated rice systems, surface-water spectral dynamics captured by NDWI accounted for nearly all predictable variation in rice vegetation condition after temporal confounds were controlled, while ensemble tree-based methods provided a marginal but consistent accuracy advantage over deep learning and linear approaches. These findings offer practical guidance for selecting robust GeoAI models and spectral predictors for satellite-based rice monitoring in irrigated agricultural landscapes.

Keywords: GeoAI, Rice, Vegetation, Acadia, Louisiana

Introduction

Rice is a major staple food for nearly two-thirds of the world's population and supports the livelihoods of more than 144 million smallholder farmers worldwide, accounting for approximately 13% of the annual global crop value (Verma et al., 2021; Asma et al., 2023; Rahman et al., 2025). However, rice production is increasingly affected by climate variability, which accounts for an

estimated 32–39% of global yield variability (Ray et al., 2015; Asma et al., 2023; Rahman et al., 2025). Effective monitoring of crop condition has therefore become essential for supporting timely agricultural management and improving production resilience. However, in many rice-growing regions, sparse ground observations and limited monitoring infrastructure constrain the timely assessment of crop conditions (Macedo et al., 2024; Gyan et al., 2025; Xiao et al., 2025). These limitations highlight the need for scalable, satellite-based monitoring approaches capable of providing consistent information over large agricultural landscapes.

Remote sensing has become an essential tool for agricultural monitoring by providing repeated, spatially continuous observations of crop conditions over large geographic areas (Gyan et al., 2025; Xiao et al., 2025). Among the available satellite platforms, the Landsat program offers one of the longest continuous Earth observation records, making it particularly valuable for monitoring long-term changes in vegetation condition and agricultural systems (Wulder et al., 2019; Zhu et al., 2019). Spectral vegetation indices derived from Landsat imagery, such as the Normalized Difference Vegetation Index (NDVI), provide reliable measures of canopy greenness and vegetation vigor and have been widely used to monitor crop growth and environmental stress (Gao, 1996; Tornos et al., 2015; Shojaeezadeh et al., 2025). Water-sensitive spectral indices, including the Normalized Difference Water Index (NDWI) and the Normalized Difference Moisture Index (NDMI), provide complementary information on surface inundation and vegetation water status, making them particularly valuable for monitoring the phenological development of flood-irrigated rice systems (Boschetti et al., 2014; Tornos et al., 2015; Chen et al., 2026). Integrating these remotely sensed observations with environmental variables, including rainfall, temperature, and terrain, provides a more comprehensive representation of the factors influencing crop condition. However, combining multi-source satellite and environmental datasets remains challenging because of differences in spatial resolution, temporal synchronization, and radiometric characteristics (Bazrafkan et al., 2025). These challenges highlight the need for robust analytical approaches capable of effectively integrating diverse geospatial datasets for agricultural monitoring.

To address the challenges of integrating multi-source remotely sensed and environmental data, machine learning (ML) and deep learning (DL) techniques have become increasingly important in agricultural remote sensing because of their ability to model complex, non-linear relationships that are difficult to capture using conventional statistical approaches (Kamilaris & Prenafeta-Boldú, 2018; Mahendra et al., 2022; Kavipriya & Vadivu, 2024). Ensemble learning methods and neural network models have demonstrated strong predictive performance for crop monitoring by integrating spectral indices with environmental variables to characterize vegetation responses under varying climatic conditions (Kavipriya & Vadivu, 2024; Nossam et al., 2024). Deep learning approaches are particularly advantageous when high-dimensional imagery is available because they can learn complex spatial features directly from image data (Bellis et al., 2022). Despite these advances, most studies evaluate only a limited number of algorithms, making it difficult to determine which modelling approaches perform most consistently across different environmental settings. Furthermore, challenges related to large training-data requirements, limited model interpretability, and the scarcity of high-quality benchmark datasets continue to constrain the broader application and generalizability of these methods (Joshi et al., 2023; Kanaparthy & Venkatesan, 2025; Liu, 2024).

A key limitation of conventional machine learning and deep learning approaches is their limited representation of geospatial context. While conventional ML and DL models effectively capture

spectral and temporal patterns, they do not explicitly account for the spatial dependencies and environmental heterogeneity that characterize geospatial data, including soil variability, topographic gradients, microclimatic differences, and spatial autocorrelation (Nikparvar & Thill, 2021; Jemeļjanova et al., 2024). Ignoring these spatial relationships can lead to biased or less reliable predictions (Yun & Gramig, 2022). In contrast, models that explicitly incorporate spatial information through geographically weighted regression, spatial error structures, or graph-based learning have frequently demonstrated improved predictive performance over conventional aspatial approaches (You et al., 2017; Khan et al., 2022; Wang et al., 2024). GeoAI extends this capability by integrating artificial intelligence with geographically referenced data, enabling predictive models to better represent the spatial processes that influence crop responses (Zhang et al., 2023; Liu, 2024). This integration supports more accurate and spatially explicit agricultural monitoring, providing valuable information for crop management and regional planning (Macedo et al., 2024; Soni, 2025).

Despite considerable advances in remote sensing, machine learning, and GeoAI for agricultural applications, limited research has systematically compared the performance of multiple machine learning and deep learning models for predicting rice vegetation condition using long-term satellite observations integrated with environmental variables. Existing studies have predominantly focused on evaluating individual machine learning algorithms, short-term prediction periods, or crop yield estimation, providing comparatively limited evidence on the relative performance of multiple modelling approaches for long-term vegetation monitoring (Van Klompenburg et al., 2020; Ganie et al., 2026; Vashisth et al., 2026). Addressing this gap, this study evaluates and compares multiple machine learning, deep learning, and GeoAI models for predicting rice vegetation condition, represented by the NDVI, using Landsat-derived spectral indices and environmental variables (rainfall, temperature, terrain, and field characteristics) from 2008 to 2025 in Acadia Parish, Louisiana. Specifically, the study (1) compares the predictive performance of competing modelling approaches, (2) quantifies the relative importance of environmental predictor variables, and (3) situate the predictive modelling results within a broader GeoAI framework for scalable, satellite-based agricultural monitoring. Model performance is assessed using RMSE, MAE, and R^2 (Huan et al., 2025; Karongo et al., 2025). By providing a comprehensive long-term comparison of predictive modelling approaches and their key environmental drivers, this study offers practical guidance for selecting robust GeoAI models for satellite-based agricultural monitoring and decision support in rice-growing regions.

Materials and Methods

Study Area

Acadia Parish, located in the rice belt of southwestern Louisiana, was selected as the study area because of its long-standing and continuing importance to the state's rice economy. In 2025, the parish cultivated approximately 84,000 acres of rice alongside soybeans, crawfish, and sugarcane, making it one of the state's leading rice-producing parishes (LSU AgCenter, 2025). Rice production in southwest Louisiana parishes such as Acadia has for decades represented a substantial share of the state's total acreage and farm-gate value, with associated production costs and returns tracked annually by LSU AgCenter economists (Deliberto & Salassi, 2010). The parish's flat topography, clay-rich prairie soils, and reliance on flood irrigation support extensive rice cultivation. It produces the strong seasonal interactions among vegetation growth, surface water inundation, and temperature that make satellite-based monitoring both feasible and informative (Deliberto & Salassi, 2010;

Kennedy et al., 2022). Because rice fields in the parish frequently shift in location and extent from year to year due to crop rotation and changing land-management decisions, static or infrequent land-cover assessments cannot reliably capture actual planting patterns. Annual, field-level mapping is therefore necessary to track where and how rice is grown over time. The parish's broad and relatively concentrated distribution of rice fields makes it a practical setting for integrating vegetation and moisture indices derived from satellite imagery with rainfall, temperature, and terrain data to characterize both crop condition and the environmental drivers of yield variability.

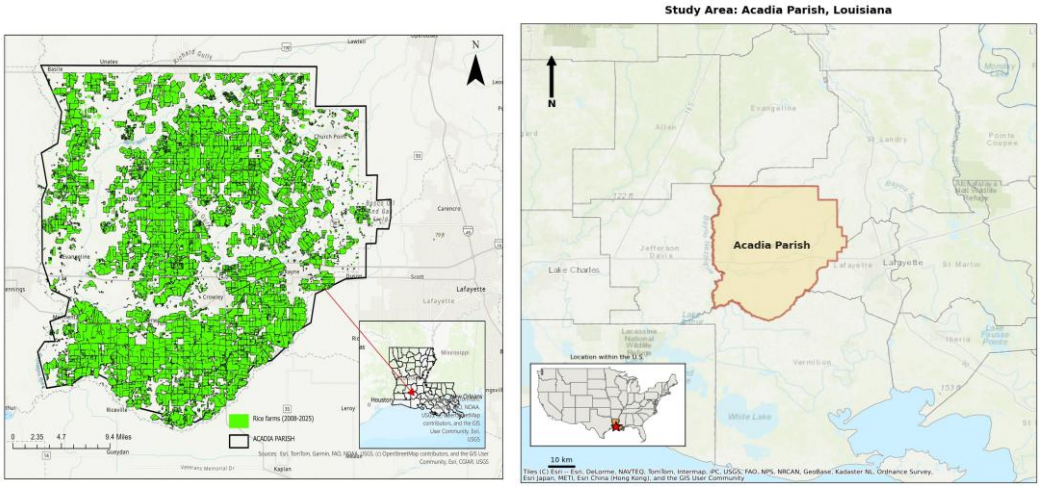


Fig. 1 *Study area maps showing the location of Acadia Parish in Louisiana, USA (right), and the spatial distribution of annual USDA Cropland Data Layer (CDL)-derived rice fields used in the analysis from 2008 to 2025 (left)*

Data Sources

The study integrated crop-cover, satellite, climate, and terrain datasets to examine rice-field conditions in Acadia Parish, Louisiana, from 2008 to 2025. Annual rice areas were derived from the USDA National Agricultural Statistics Service (USDA-NASS) Cropland Data Layer (CDL) using the rice class (Class 3). Because the CDL represents classified crop cover at the pixel level rather than cadastral boundaries, the extracted rice areas were treated as CDL-derived rice polygons (Lark et al., 2021). Landsat Collection 2 Level-2 surface-reflectance imagery provided the multispectral observations used to characterize monthly vegetation and moisture conditions (USGS 2025). Landsat 5 Thematic Mapper imagery was used for 2008-2011, Landsat 7 Enhanced Thematic Mapper Plus imagery for 2012, Landsat 8 Operational Land Imager imagery for 2013-2021, and a merged Landsat 8-9 collection for 2022-2025 to ensure continuous satellite observations throughout the study period. These datasets provide atmospherically corrected surface-reflectance bands and accompanying quality-assurance information suitable for long-term terrestrial monitoring. Monthly rainfall and 2-m air temperature were obtained from the ERA5-Land reanalysis dataset, using monthly total precipitation and monthly mean 2-m air temperature as climate variables (Muñoz-Sabater et al., 2021). Terrain slope was derived from the void filled CGIAR Shuttle Radar Topography Mission (SRTM) digital elevation model, which has an approximate spatial resolution of 90m (Farr et al., 2007). All image preprocessing, dataset integration, and variable extraction were conducted in Google Earth Engine (Gorelick et al., 2017).

Data Extraction

Annual rice masks were extracted separately for each year from 2008 to 2025. Each CDL image was clipped to the Acadia Parish boundary, and all non-rice pixels were removed through binary reclassification and self-masking. To reduce isolated classification noise, a connected-pixel operation was applied, and rice patches containing fewer than three connected pixels were removed (Lv et al., 2017). The cleaned rice raster was subsequently converted to polygon features at a nominal spatial resolution of 30m. Polygon area was calculated in hectares and features smaller than 1 ha were excluded. Each retained polygon was assigned its corresponding observation year and a unique identifier following the structure *ACADIA_year_PolygonID*. This process produced a separate annual rice-polygon layer, thereby allowing the spatial configuration of cultivated rice to vary between years rather than if the same fields remained in production throughout the study period.

Four spectral indices were calculated for every monthly Landsat composite. The NDVI was calculated from the near-infrared and red bands to represent vegetation greenness and canopy development. The Enhanced Vegetation Index (EVI) incorporated the near-infrared, red, and blue bands to improve sensitivity under relatively dense vegetation conditions. The Normalized Difference Moisture Index (NDMI) was calculated from the near-infrared and first shortwave-infrared bands to represent canopy and vegetation moisture conditions, while the Normalized Difference Water Index (NDWI) used the green and near-infrared bands to indicate surface wetness and open-water influence. The formulas implemented were:

$$NDVI = (NIR - R) / (NIR + R) \quad (1)$$

$$NDWI = (G - NIR) / (G + NIR) \quad (2)$$

$$EVI = G * ((NIR - R) / (NIR + C1 * R – C2 * B + L)), \text{ where.} \quad (3)$$

$$NDMI = (NIR - SWIR)/ (NIR + SWIR) \quad (4)$$

where NIR, R, G, B, and $SWIR_1$ represent the near-infrared, red, green, blue, and first shortwave infrared reflectance bands, respectively. For EVI, G is the gain factor (2.5), C_1 and C_2 are the aerosol resistance coefficients (6.0 and 7.5, respectively), and L is the canopy background adjustment factor (1.0) (Huete et al., 2002).

The monthly spectral-index images, temperature layer, rainfall layer, and slope layer were combined into a multiband image for each year combination. Mean values were then calculated within every annual rice polygon using zonal reduction. The final dataset therefore contained one observation for each unique combination of rice polygon and year. The exported attributes included rice-field identifier, year, month, polygon area, NDVI, EVI, NDMI, NDWI, monthly rainfall, monthly mean temperature, and mean slope. The results were exported from Google Earth Engine as a single CSV file for subsequent machine learning and deep learning analysis in Python.

Data Preprocessing

Landsat Collection 2 Level-2 surface-reflectance digital numbers were converted to scaled surface reflectance using the recommended multiplicative factor (0.0000275) and additive offset (−0.2), following the USGS Collection 2 Level-2 specifications (USGS, 2025). The spectral bands from Landsat 5 and 7 were renamed to blue, green, red, nir, swir1, and swir2. Equivalent spectral bands from Landsat 8 and 9 were assigned the same standardized names. This standardization allowed the

same spectral-index functions to be applied across the different Landsat sensors. Cloud and invalid-pixel screening was performed using the Landsat *QA_PIXEL* band. Following the USGS Landsat Collection 2 QA band definition, the bitwise quality mask removed pixels flagged within bits 0-4, corresponding to fill, dilated cloud, cloud, or cirrus, and cloud shadow. The mask was applied before spectral indices were calculated. Monthly median composites were generated from all available cloud-masked Landsat observations to minimize the influence of residual atmospheric contamination and anomalous pixel values while providing a representative estimate of rice-field conditions for each month.

All spectral variables were extracted at a nominal 30m processing scale, corresponding to Landsat optical resolution. The SRTM slope layer had a native resolution of approximately 90 m, while ERA5-Land climate variables were substantially coarser, at roughly 9-11 km. All variables were extracted using a nominal 30 m processing scale to align the computational grid with the Landsat-derived rice polygons. This extraction scale did not increase the native spatial resolution of the SRTM (approximately 90 m) or ERA5-Land climate data (approximately 9–11 km), which retained their original spatial characteristics. The exported CSV was structured in long format, with repeated monthly observations nested within annual rice polygons. Slope remained constant within each polygon across months, whereas rainfall, temperature, and spectral indices varied temporally.

Variables for Analysis

The NDVI, expressed as a single seasonal composite value per field season, was used as the dependent variable and proxy for rice growth. Six independent variables were considered: field area (area_ha), the NDMI, the NDWI, cumulative growing-season rainfall (rain_mm_gs), mean growing-season temperature (temp_c_gs), and terrain slope (slope_deg). The growing season was defined as April to September to correspond with the typical rice cultivation calendar in Acadia Parish (Levy et al., 2025).

Table 1 Variables used in the analysis, their role, and units.

Variable	Role	Unit	Min	Max	SD
NDVI	Dependent	Unitless (-1 to 1)	-0.182	0.872	0.115
year	Confound (control)	Calendar year	2008	2025	-
area_ha	Predictor	Hectares	1.08	2508.18	83.30
NDMI	Predictor	Unitless (-1 to 1)	-0.155	0.696	0.111
NDWI	Predictor	Unitless (-1 to 1)	-0.781	0.212	0.083
rain_mm_gs	Predictor	mm	418.61	1376.27	194.84
temp_c_gs	Predictor	°C	23.12	26.26	0.70
slope_deg	Predictor	Degrees	0.00	5.35	0.41

Note: NDVI = Normalized Difference Vegetation Index (proxy for rice vegetation condition); NDMI = Normalized Difference Moisture Index; NDWI = Normalized Difference Water Index; Area_ha = rice

field area (hectares); Rain_mm_gs = cumulative growing-season rainfall; Temp_c_gs = mean growing-season temperature; Slope_deg = terrain slope. Year was included as a control variable to account for temporal variation.

Control for a temporal confound

Growing-season year was treated as a potential confounding variable rather than a direct predictor of NDVI (Table 1). Although year does not directly influence rice growth, it captures unmeasured temporal factors such as long-term climate variability, sensor differences, and changes in agronomic practices. Treating year as a conventional predictor could therefore confound the relationships between NDVI and the environmental variables by attributing shared temporal variation to individual predictors. To control for shared year-to-year variation, a year fixed-effects (demeaning) procedure was applied. For each variable of interest (NDVI and the six predictor variables), the year-specific mean was subtracted from each observation:

$$x'_{i,t} = x_{i,t} - \bar{x}_t \quad (5)$$

where $x_{i,t}$ is the value of variable x for field i in year t, and $\bar{x}_t$ is the mean of that variable across all fields in year t. This transformation was applied to the full dataset to remove shared annual variation before model fitting, allowing the analysis to focus on within-year differences among rice fields (Wooldridge, 2010).

Model development

Six machine learning algorithms and one deep learning architecture were fitted to the year-adjusted data: linear regression, ridge regression (L2 penalty, $\alpha = 1.0$), random forest regression (400 trees, maximum depth 10, minimum 5 samples per leaf), gradient boosting regression (300 estimators, maximum depth 3, learning rate 0.05), extreme gradient boosting (XGBoost; 400 estimators, maximum depth 4, learning rate 0.05, subsample and column-sample fractions of 0.8), and light gradient boosting machine (LightGBM; equivalent settings to XGBoost). The deep learning model was a feed-forward multilayer perceptron with three hidden layers (128, 64, and 32 units respectively), rectified linear unit (ReLU) activations, L2 regularization ($\alpha = 1 \times 10^{-4}$), and the Adam optimizer (initial learning rate 1×10^{-3}). The neural network used z-score standardized inputs, with scaling parameters estimated separately within each training fold to prevent information leakage. Linear and ridge regression were fit on unstandardized input because ordinary least squares is invariant to linear rescaling and ridge regression showed negligible sensitivity to scaling at the regularization strength used ($\alpha = 1.0$), this did not materially affect the reported results. For the neural network, a 15% inner validation split was held out from each training fold for early stopping: training was halted if validation loss failed to improve for 20 consecutive epochs, and the model weights from the epoch with the lowest validation loss were retained for evaluation on that fold's test partition.

Model evaluation

Because the analytical objective was explanatory, to quantify whether environmental and site variables explain within-year variation in rice growth after controlling for the year confound, rather than to forecast unobserved future seasons, model performance was assessed using five-fold random cross-validation rather than a chronological (time-ordered) hold-out split. This distinction was methodologically necessary: year fixed-effects are computed from each year's own mean, a quantity that is not available in advance in a genuine forecasting context, so a chronological hold-

out would not constitute a fair forecast evaluation once year fixed-effects are applied. Random k-fold cross-validation avoids this issue and is the standard evaluation approach for explanatory panel-data models. For each fold, models were trained on four-fifths of the data and evaluated on the held-out fifth; this was repeated five times so that every observation was used for testing exactly once. Performance was quantified using the coefficient of determination (R^2), root mean squared error (RMSE), and mean absolute error (MAE), each reported as the mean and standard deviation across the five folds. To characterize which variables contributed to model predictions, two complementary approaches were used. First, impurity-based feature importance was extracted from the random forest and XGBoost models. Second, and more conservatively, permutation importance was computed on an independent 80/20 held-out split: each predictor was randomly shuffled in turn, and the resulting mean decrease in R^2 (relative to the unpermuted baseline), averaged over 20 repetitions, was taken as a model-agnostic measure of that variable's contribution to predictive accuracy. All the analyses conducted in this study was run using python via VS Code.

Results

Descriptive patterns and correlation structure

Across the 18-year study period (2008–2025; n = 12,544 field-seasons), NDVI exhibited weak unadjusted correlations with field area (r = 0.054), cumulative growing-season rainfall (r = 0.071), mean growing-season temperature (r = 0.057), and terrain slope (r = 0.071). In contrast, NDVI was strongly negatively correlated with NDWI (r = −0.963) and moderately positively correlated with NDMI (r = 0.445) (Fig. 2).

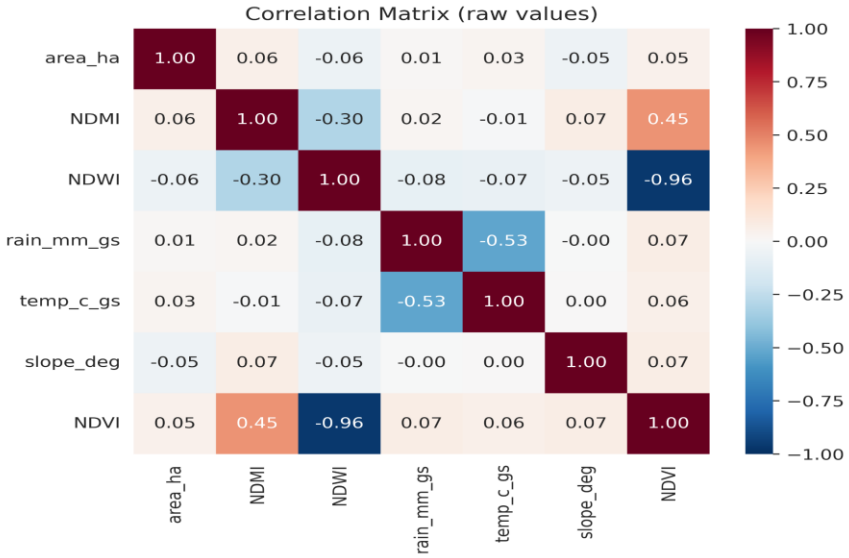


Fig. 2 Correlation matrix among NDVI and candidate predictor variables

Annual parish-wide averages of NDVI, cumulative growing-season rainfall, mean growing-season temperature, and NDMI varied across the 2008–2025 study period (Fig. 3). Mean NDVI ranged from approximately 0.48 to 0.63, with comparatively higher values observed in 2015, 2018, and 2024–2025. Growing-season rainfall exhibited substantial year-to-year variability, ranging from about 480 mm to more than 1,200 mm. Mean growing-season temperature varied within a relatively narrow range (approximately 24.2–26.0 °C), while annual mean NDMI fluctuated between approximately 0.16 and 0.29 throughout the study period.

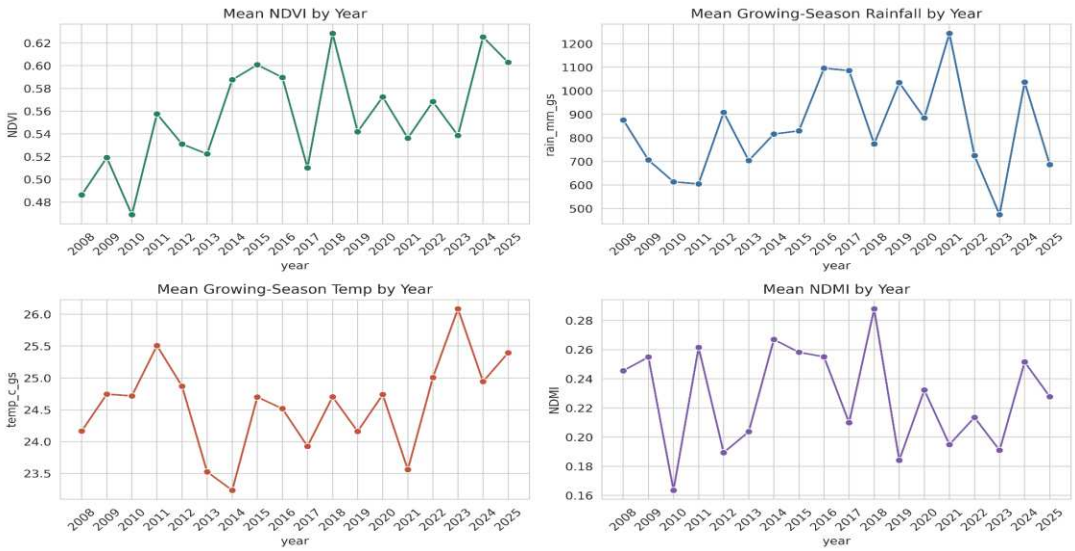


Fig. 3 Parish-wide annual means of NDVI, growing-season rainfall, growing-season temperature, and NDMI, 2008–2025

Model performance after controlling for the year confound

Following removal of the year-specific mean from NDVI and each predictor (year fixed-effects; see Materials and Methods), seven models were evaluated using five-fold random cross-validation. Gradient Boosting achieved the highest predictive performance (R^2 = 0.960 ± 0.002). Linear regression (R^2 = 0.948 ± 0.003) and ridge regression (R^2 = 0.947 ± 0.003) produced the lowest coefficients of determination. Similar patterns were observed for RMSE and MAE, with Gradient Boosting yielding the lowest RMSE (0.0211), while LightGBM and XGBoost achieved the lowest MAE (0.0153). The linear models produced the highest RMSE (0.0242) and MAE (0.0170–0.0172) values (Table 2). Standard deviations of R^2 across the five cross-validation folds were ≤ 0.004 for all models.

Table 2 Five-fold cross-validation performance of the evaluated machine learning and deep learning models.

Model	R^2 (mean ± SD)	RMSE (mean)	MAE (mean)
Gradient Boosting	0.960 ± 0.002	0.0211	0.0154
LightGBM	0.959 ± 0.004	0.0215	0.0153
Random Forest	0.959 ± 0.003	0.0215	0.0155
XGBoost	0.958 ± 0.004	0.0215	0.0153
Deep neural network (MLP)	0.956 ± 0.002	0.0221	0.0161
Linear regression	0.948 ± 0.003	0.0242	0.0170
Ridge regression	0.947 ± 0.003	0.0242	0.0172

Variable contribution

Impurity-based feature importance derived from the Random Forest and XGBoost models identified NDWI as the most influential predictor, followed by NDMI, while field area, cumulative growing-

season rainfall, mean growing-season temperature, and slope contributed comparatively little to model predictions (Fig. 4).

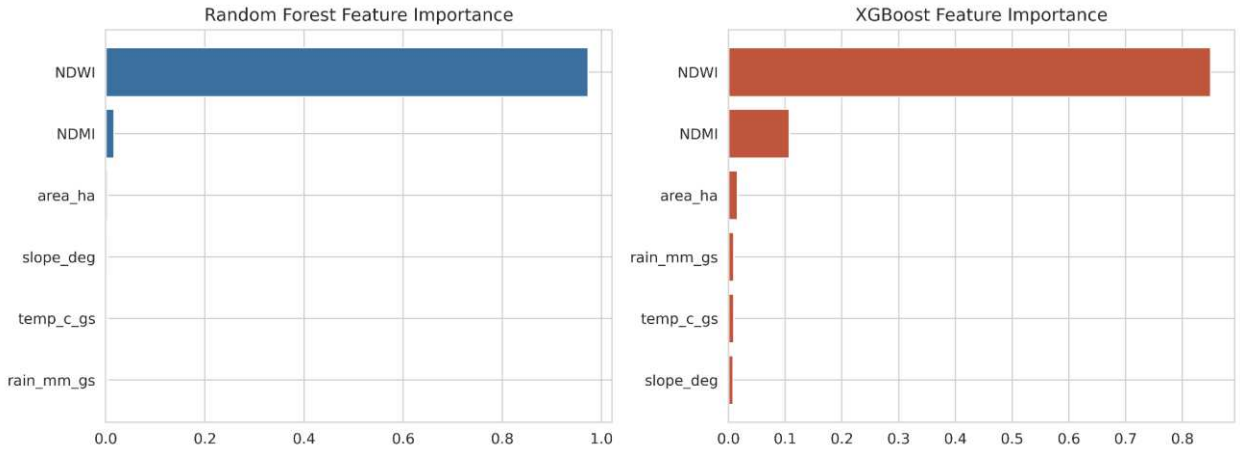


Fig. 4 Impurity-based feature importance derived from the Random Forest (left) and XGBoost (right) models

Permutation importance was subsequently evaluated using an independent 80/20 hold-out dataset to verify the impurity-based rankings (Strobl et al., 2007). The permutation analysis produced the same ordering, with NDWI resulting in the largest reduction in model performance ($\Delta R^2 = 1.708$). Field area ($\Delta R^2 = 0.002$), mean growing-season temperature ($\Delta R^2 = 0.0008$), slope ($\Delta R^2 = 0.0004$), and cumulative growing-season rainfall ($\Delta R^2 = 0.0002$) each produced only minimal reductions in R^2 when permuted (Table 3; Fig. 5).

Table 3 Permutation feature importance of predictor variables based on the mean decrease in R^2 over 20 repetitions using an independent hold-out dataset.

Predictor	**Permutation importance (ΔR^2)**
NDWI	1.708
NDMI	0.034
area_ha	0.002
temp_c_gs	0.0008
slope_deg	0.0004
rain_mm_gs	0.0002

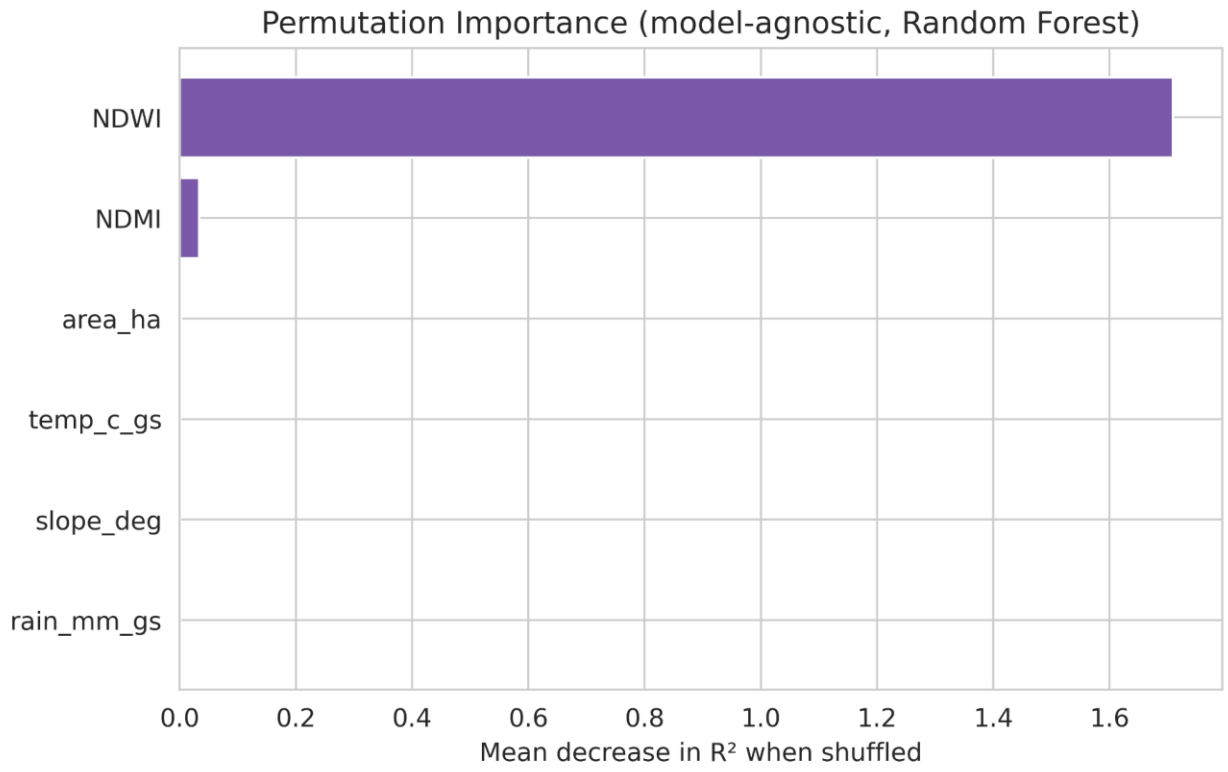


Fig. 5 Permutation feature importance showing the mean decrease in R^2 following predictor shuffling on an independent hold-out dataset

Deep learning behavior and predictive fit

Training and validation loss decreased rapidly during the initial training epochs before gradually stabilizing (Fig. 6). Throughout training, validation loss remained consistently higher than training loss, while both curves followed similar trajectories and reached a near-plateau after approximately 15–20 epochs. Across the five cross-validation folds, no model met the 20-epoch early stopping criterion before completion of the maximum training epochs. The deep neural network achieved a mean cross-validated performance of $R^2 = 0.956 \pm 0.002$ (Table 2).

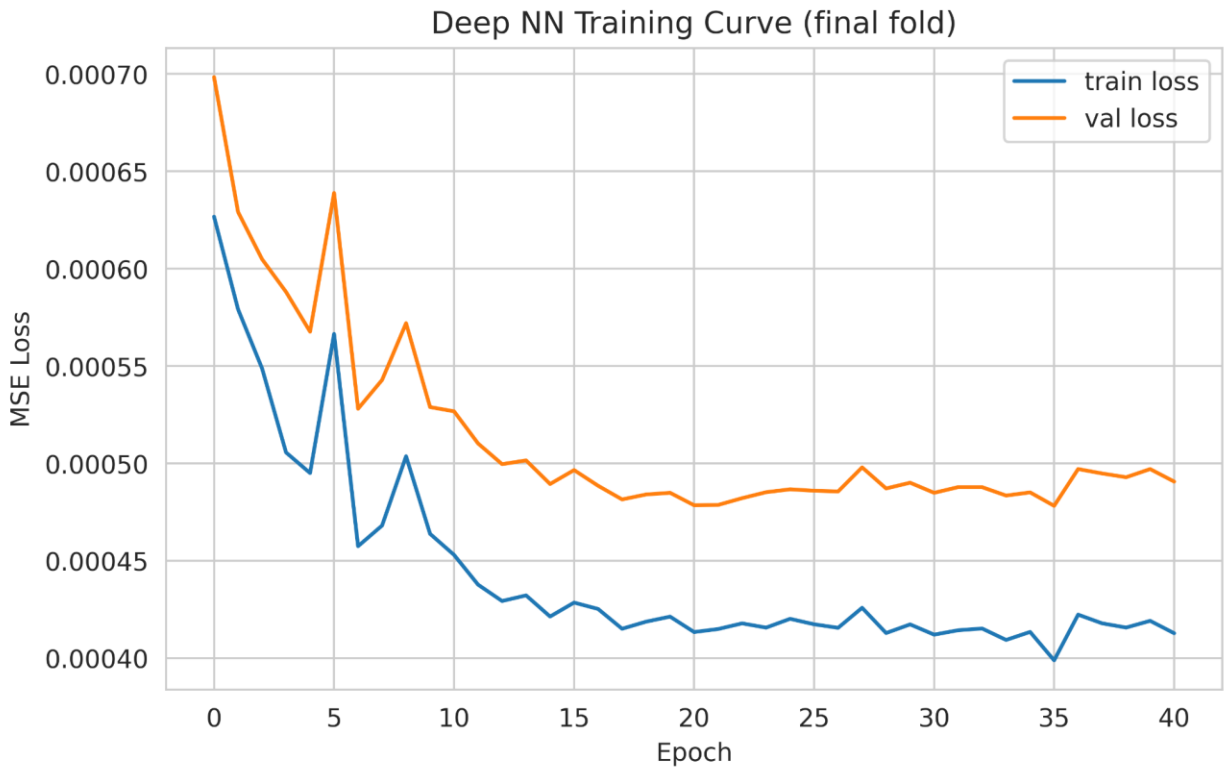


Fig. 6 Training and validation loss curves for the deep neural network during the final cross-validation fold

Predicted versus observed year-adjusted NDVI values for the Random Forest model showed close agreement with the 1:1 reference line across the range of observations (Fig. 7). Most predictions were tightly clustered around the diagonal, with no evident systematic overprediction or underprediction. A small number of observations deviated from the reference line, particularly at lower year-adjusted NDVI values. The model achieved a hold-out coefficient of determination (R^2) of 0.960.

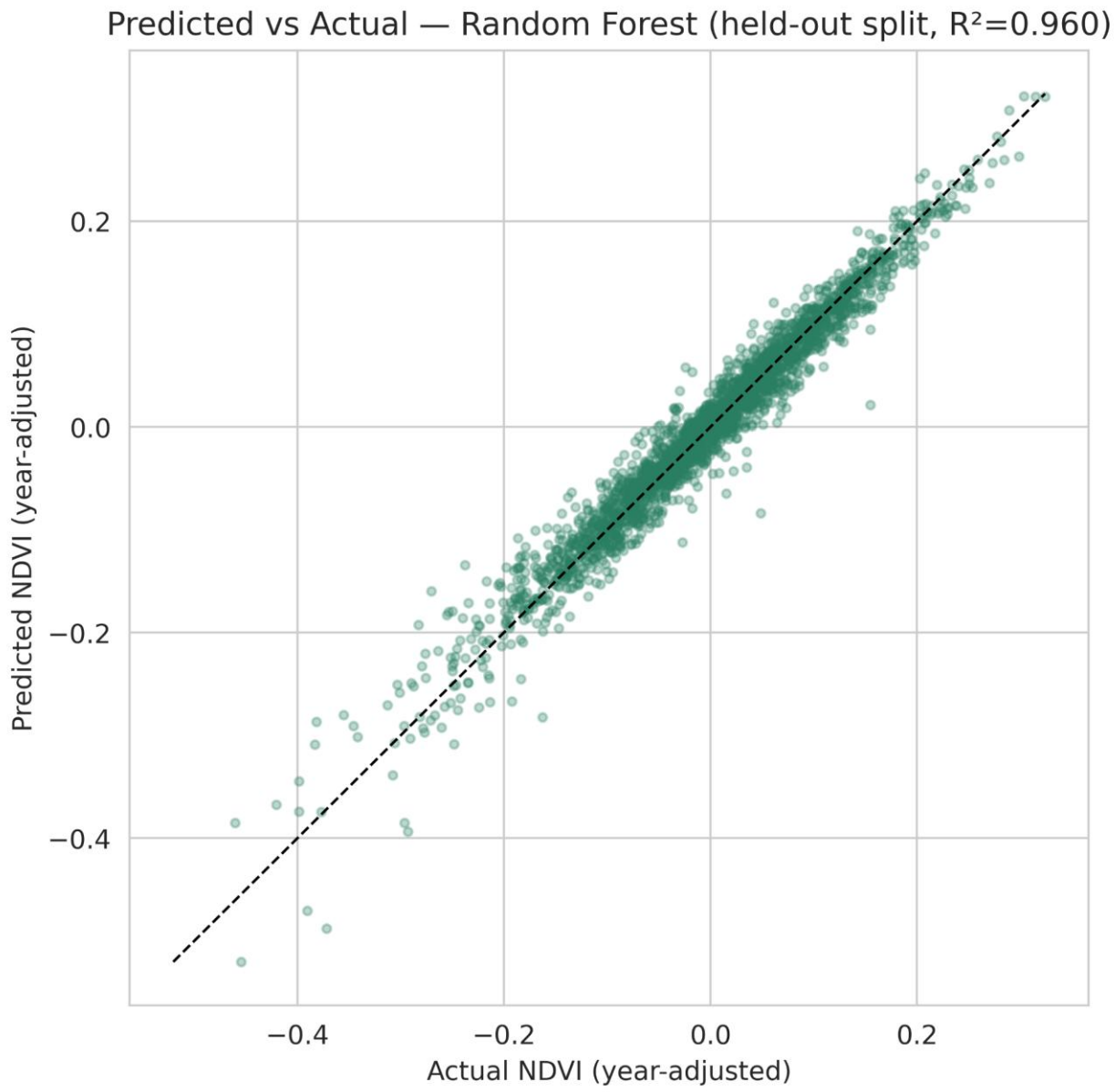


Fig. 7 Observed versus predicted year-adjusted NDVI values for the Random Forest model on the independent hold-out dataset. The dashed line represents the 1:1 reference line

Discussion

Relationships between rice vegetation condition and predictor variables

The strong negative relationship between NDVI and NDWI (r = −0.963) reflects the characteristic phenology of flood-irrigated rice systems, where early-season flooding produces high NDWI and low NDVI, followed by increasing vegetation greenness and declining surface water as the crop develops. This inverse relationship has been widely reported as a distinctive spectral signature of paddy rice, with NDWI effectively capturing flooding and transplanting while NDVI tracks canopy development (Tornos et al., 2015; Xiao et al., 2025). In contrast, the moderate positive correlation between NDVI and NDMI (r = 0.445) is consistent with NDMI's sensitivity to vegetation water content, reflecting changes in canopy moisture as rice develops (Gao, 1996). Together, these findings suggest that NDWI

and NDMI provide complementary information on rice water dynamics by representing surface inundation and canopy moisture, respectively. The weak relationships between NDVI and field area, rainfall, temperature, and slope indicate that these variables explained relatively little of the observed variation in rice vegetation condition, likely reflecting the controlled hydrological conditions of irrigated rice production in Acadia Parish and the relatively small variation in growing-season temperature during the study period.

Comparative performance of the evaluated prediction models

The ensemble tree-based models achieved the highest predictive performance, with Gradient Boosting (R^2 = 0.960), LightGBM (R^2 = 0.959), Random Forest (R^2 = 0.959), and XGBoost (R^2 = 0.958) performing marginally better than the deep neural network (R^2 = 0.956) and the linear models (R^2 = 0.947–0.948). Although the differences were small (ΔR^2 = 0.013), the consistent ranking indicates that ensemble methods provided the most accurate representation of the nonlinear relationships between the spectral and environmental variables and rice vegetation condition. This finding agrees with previous studies demonstrating that ensemble learning methods consistently achieve high predictive performance for agricultural remote sensing applications because of their ability to model complex feature interactions while maintaining robustness across different environmental conditions (Kamilaris & Prenafeta-Boldú, 2018; Mahendra et al., 2022; Kavipriya & Vadivu, 2024). The slightly lower performance of the deep neural network also agrees with previous studies suggesting that deep learning models generally require larger training datasets and greater parameter optimization to consistently outperform ensemble methods on structured tabular data (Joshi et al., 2023; Liu, 2024; Kanaparthy & Venkatesan, 2025). However, the comparatively lower performance of the linear and ridge regression models reflects their limited ability to capture nonlinear relationships and complex interactions among predictor variables. Nevertheless, their relatively high predictive accuracy suggests that a substantial proportion of the within-year variation in rice vegetation condition remained approximately linear after year-level demeaning, indicating that simpler and more interpretable models may still provide acceptable performance when computational efficiency and model transparency are priorities.

Importance of water-related spectral indices for rice vegetation prediction

The overwhelming importance of NDWI, which produced the largest permutation importance (ΔR^2 = 1.708), far exceeding NDMI (ΔR^2 = 0.034) and all other predictors ($\Delta R^2 \leq 0.002$), highlights the dominant role of surface-water dynamics in predicting rice vegetation condition. This finding is consistent with the hydrological characteristics of flood-irrigated rice systems, where managed flooding governs early crop establishment before canopy development progressively replaces the open-water signal. Consequently, NDWI effectively captures the seasonal transition from flooded fields to dense vegetation, making it the strongest predictor of NDVI. Although NDMI also reflects crop water status, its substantially lower importance indicates that surface inundation provided more predictive information than canopy moisture under the conditions of this study. Similar findings have been reported by Boschetti et al. (2014), who demonstrated that water-sensitive spectral indices are among the most reliable indicators of managed flooding and rice phenology in paddy systems, while Chen et al. (2026) further showed that integrating NDWI with vegetation indices effectively captures the temporal and spatial dynamics of rice growth. The comparatively small contributions of rainfall, temperature, slope, and field area are likely attributable to the controlled irrigation practices in Acadia Parish, the relatively uniform topography, and the removal of shared

interannual variability through the year-demeaning procedure. These findings do not suggest that environmental variables are unimportant for rice production; rather, they indicate that, within individual growing seasons, the water-related spectral information captured by NDWI provided substantially greater predictive value than the broader environmental variables considered in this study.

Deep learning performance relative to ensemble methods

The deep neural network achieved high predictive performance (R^2 = 0.956) but remained marginally below the ensemble tree-based models, particularly Gradient Boosting (R^2 = 0.960). This finding agrees with previous studies showing that, for structured tabular datasets with well-engineered predictors, ensemble learning methods often perform as well as or better than deep learning models because they effectively capture nonlinear relationships without requiring large training datasets or extensive parameter optimization (Kamilaris & Prenafeta-Boldú, 2018; Mahendra et al., 2022; Kavipriya & Vadivu, 2024). The smooth convergence of the training and validation loss curves further indicates that the neural network learned the underlying relationships without substantial optimization difficulties, suggesting that its slightly lower performance was more likely related to the characteristics of the input data than to model training. Because the predictor variables were aggregated to polygon-level tabular features, the deep neural network could not exploit the spatial feature-learning capability that typically provides an advantage for image-based applications. Similar observations were reported by Bellis et al., (2022), who showed that deep learning models achieve greater improvements when applied directly to high-dimensional UAV imagery, where spatial information is preserved. These findings suggest that ensemble methods provide a practical and computationally efficient solution for rice vegetation prediction from structured geospatial datasets, whereas deep learning approaches may offer greater advantages when spatially explicit image data are used directly.

Implications for operational rice monitoring

The findings of this study demonstrate the potential of GeoAI to support operational rice monitoring by integrating long-term satellite observations with environmental information in a scalable predictive framework. The consistently high performance of the evaluated models indicates that Landsat-derived spectral indices provide reliable information for monitoring rice vegetation condition over extended periods, while the superior performance and interpretability of the ensemble tree-based models make them particularly well suited for operational decision-support applications. The dominance of NDWI further highlights the importance of water-sensitive spectral information for monitoring flood-irrigated rice systems, suggesting that routine satellite observations can effectively characterize crop development without relying extensively on auxiliary climate or terrain data under managed irrigation conditions. These findings support the use of remotely sensed spectral information as a practical and cost-effective approach for large-area rice monitoring and provide a foundation for future GeoAI applications that incorporate spatially explicit modelling approaches, such as geographically weighted machine learning, to better account for local spatial variability in crop responses (Khan et al., 2022).

Study limitations and future research

Several limitations should be considered when interpreting the findings of this study. First, rice vegetation condition was represented using NDVI, which is known to saturate under dense canopy conditions and may underestimate vegetation variability during peak growth stages. Future studies could incorporate alternative vegetation indices, such as the Enhanced Vegetation Index (EVI) or

chlorophyll-sensitive indices, to improve the characterization of dense rice canopies. Second, the year fixed-effects approach effectively removed shared interannual variability but limits the direct application of the models for predicting previously unseen growing seasons. Developing forecasting frameworks that preserve temporal variability while maintaining robust predictive performance remains an important area for future research. Third, the spatial resolution mismatch among the Landsat imagery (30 m), SRTM terrain data (approximately 90 m), and ERA5-Land climate variables (approximately 9-11 km) may have reduced the apparent contribution of terrain and climate variables to model performance. Evaluating higher-resolution environmental datasets may provide additional insight into local factors influencing rice vegetation condition. Fourth, although this study was developed within a GeoAI framework, the evaluated models did not explicitly account for spatial autocorrelation or spatial non-stationarity. Incorporating spatially explicit machine learning approaches, such as geographically weighted or graph-based models, may further improve predictive performance by capturing local spatial variability (Khan et al., 2022). Finally, the analysis was limited to Acadia Parish, Louisiana, where flood-irrigated rice production and relatively uniform topography characterize the agricultural landscape. Extending the framework to other rice-growing regions with different irrigation practices, climatic conditions, and terrain characteristics will help evaluate the generalizability of the proposed approach and identify the conditions under which different modelling strategies perform best.

Conclusion

This study evaluated seven machine learning and deep learning models, situated within a broader GeoAI framework, to characterize rice vegetation condition using 18 years (2008–2025) of Landsat-derived spectral indices and environmental variables in Acadia Parish, Louisiana. The results showed that all evaluated models achieved high predictive accuracy, with ensemble tree-based methods providing the best overall balance between prediction accuracy, computational efficiency, and interpretability. Among all predictor variables, NDWI emerged as the dominant predictor of rice vegetation condition, highlighting the critical role of surface-water dynamics in flood-irrigated rice systems, while rainfall, temperature, terrain, and field characteristics contributed comparatively little after accounting for interannual variability. These findings demonstrate the value of integrating long-term satellite observations with machine learning within a GeoAI framework for scalable agricultural monitoring and show that water-sensitive spectral information can effectively characterize rice vegetation condition under managed irrigation. This study therefore provides practical guidance for selecting robust predictive models and key environmental predictors for satellite-based rice monitoring, while establishing a foundation for future GeoAI applications that incorporate spatially explicit modelling and evaluate the transferability of these approaches across diverse rice-growing environments.

Acknowledgements

Not applicable.

Author Contributions

Desmond Fosuhene: Conceptualization, Writing – original draft, Writing – review and editing, Methodology. Dorcas Twumwaa Gyan: Conceptualization, Writing – original draft, Data curation, Writing – review and editing. Kingsford Kobina Annan: Conceptualization, Writing – original draft, Writing – review and editing. Theodora Mary Fletcher: Writing – original draft, Writing – review and editing. Bhuwan Thapa: Writing – review and editing. Ebenezer Nana Kwaku Boateng: Conceptualization, Writing – original draft, Writing – review and editing, Methodology, Formal analysis, Supervision.

ORCID

Desmond Fosuhene - https://orcid.org/0009-0005-4870-2954

Dorcas Twumwaa Gyan - https://orcid.org/0009-0005-8451-2605

Kingsford Kobina Annan - https://orcid.org/0009-0003-9693-8844

Ebenezer Nana Kwaku Boateng - https://orcid.org/0000-0002-3911-5345

Theodora Mary Fletcher - https://orcid.org/0009-0008-1276-9091

Declarations

Funding

No funding was received for conducting this study.

Competing interests

The authors have no relevant financial or non-financial interests to disclose.

Data availability

The Landsat, ERA5-Land, SRTM, and USDA Cropland Data Layer datasets analyzed during this study are publicly available from the U.S. Geological Survey, the Copernicus Climate Change Service, and the USDA National Agricultural Statistics Service, respectively, and were processed in Google Earth Engine. The derived field-season dataset generated during the current study is available from the corresponding author on reasonable request.

References

Asma, J., D, S., & D, K. (2023). The Global Lifeline: A Staple Crop Sustaining Two-Thirds of the World's Population. *Agriculture Archives*, *2*(3), 15–18. https://doi.org/10.51470/AGRI.2023.2.3.15

Bazrafkan, A., Igathinathane, C., Bandillo, N., & Flores, P. (2025). Optimizing integration techniques for UAS and satellite image data in precision agriculture—A review. *Frontiers in Remote Sensing*, *6*, 1622884. https://doi.org/10.3389/frsen.2025.1622884

Bellis, E. S., Hashem, A. A., Causey, J. L., Runkle, B. R. K., Moreno-García, B., Burns, B. W., Green, V. S., Burcham, T. N., Reba, M. L., & Huang, X. (2022). Detecting Intra-Field Variation in Rice Yield With Unmanned Aerial Vehicle Imagery and Deep Learning. *Frontiers in Plant Science*, *13*, 716506. https://doi.org/10.3389/fpls.2022.716506

Boschetti, M., Nutini, F., Manfron, G., Brivio, P. A., & Nelson, A. (2014). Comparative Analysis of Normalised Difference Spectral Indices Derived from MODIS for Detecting Surface Water in Flooded Rice Cropping Systems. *PLoS ONE*, *9*(2), e88741. https://doi.org/10.1371/journal.pone.0088741

Chen, S., Shen, B., & Shen, C. (2026). Rice yield prediction using UAV-based multispectral remote sensing and random forest machine learning algorithms. In L. Shen & F. Meng (Eds.), *Fourth International Conference on Environmental Remote Sensing and Geographic Information Technology (ERSGIT 2025)* (p. 12). SPIE. https://doi.org/10.1117/12.3096178

Deliberto, M. A., & Salassi, M. E. (2010). *Hybrid rice production costs and returns: Comparisons with conventional & Clearfield varieties* (Staff Report No. 2010-06). LSU AgCenter, Baton Rouge, LA. https://www.lsuagcenter.com/topics/crops/rice/publications/hybrid-rice-production-costs-and-returns-comparisons-with-conventional--clearfield-varieties

Farr, T. G., Rosen, P. A., Caro, E., Crippen, R., Duren, R., Hensley, S., et al. (2007). The Shuttle Radar Topography Mission. *Reviews of Geophysics*, *45*(2), 2005RG000183. https://doi.org/10.1029/2005RG000183

Ganie, M. W., Wani, M. A., & Wani, A. H. (2026). Machine learning approaches for crop yield prediction: A systematic literature review. *Remote Sensing Applications: Society and Environment*, *43*, 102151. https://doi.org/10.1016/j.rsase.2026.102151

Gao, B. (1996). NDWI—A normalized difference water index for remote sensing of vegetation liquid water from space. *Remote Sensing of Environment*, *58*(3), 257–266. https://doi.org/10.1016/S0034-4257(96)00067-3

Gorelick, N., Hancher, M., Dixon, M., Ilyushchenko, S., Thau, D., & Moore, R. (2017). Google Earth Engine: Planetary-scale geospatial analysis for everyone. *Remote Sensing of Environment*, *202*, 18–27. https://doi.org/10.1016/j.rse.2017.06.031

Gyan, D. T., Twumasi, Y. A., Ning, Z. H., Dadzie, E., Osei, J. D., Aniewu, D., et al. (2025). Geospatial Assessment of Agricultural Productivity in Jefferson Davis Parish: A Focus on Rice Cultivation. *The International Archives of the Photogrammetry, Remote Sensing and Spatial Information Sciences*, *XLVIII-M-5–2024*, 45–52. https://doi.org/10.5194/isprs-archives-XLVIII-M-5-2024-45-2025

Huete, A., Didan, K., Miura, T., Rodriguez, E. P., Gao, X., & Ferreira, L. G. (2002). Overview of the radiometric and biophysical performance of the MODIS vegetation indices. *Remote Sensing of Environment*, *83*(1–2), 195–213. https://doi.org/10.1016/S0034-4257(02)00096-2

Jemeļjanova, M., Kmoch, A., & Uuemaa, E. (2024). Adapting machine learning for environmental spatial data—A review. *Ecological Informatics*, *81*, 102634. https://doi.org/10.1016/j.ecoinf.2024.102634

Joshi, A., Pradhan, B., Gite, S., & Chakraborty, S. (2023). Remote-Sensing Data and Deep-Learning Techniques in Crop Mapping and Yield Prediction: A Systematic Review. *Remote Sensing*, *15*(8), 2014. https://doi.org/10.3390/rs15082014

Kamilaris, A., & Prenafeta-Boldú, F. X. (2018). Deep learning in agriculture: A survey. *Computers and Electronics in Agriculture*, *147*, 70–90. https://doi.org/10.1016/j.compag.2018.02.016

Kanaparthy, P. B., & Venkatesan, A. (2025). A Survey on Agricultural Precision with Deep Learning-Driven Satellite Image Analysis: A Multi-Temporal, Multi-Spectral Approach. *2025 8th International Conference on Computing Methodologies and Communication (ICCMC)*, 591–598. https://doi.org/10.1109/ICCMC65190.2025.11140702

Kavipriya, J., & Vadivu, G. (2024). Exploring Crop Yield Prediction with Remote Sensing Imagery and AI. *2024 International Conference on Advances in Computing, Communication and Applied Informatics (ACCAI)*, 1–5. https://doi.org/10.1109/ACCAI61061.2024.10601854

Kennedy, P. L., Schmitz, A., Linscombe, S., & Zhang, F. (2022). The impact of cultivar development and cultural practices on Louisiana rice yield. *Agrosystems, Geosciences & Environment*, *5*(1), e20231. https://doi.org/10.1002/agg2.20231

Khan, S. N., Li, D., & Maimaitijiang, M. (2022). A Geographically Weighted Random Forest Approach to Predict Corn Yield in the US Corn Belt. *Remote Sensing*, *14*(12), 2843. https://doi.org/10.3390/rs14122843

Lark, T. J., Schelly, I. H., & Gibbs, H. K. (2021). Accuracy, Bias, and Improvements in Mapping Crops and Cropland across the United States Using the USDA Cropland Data Layer. *Remote Sensing*, *13*(5), 968. https://doi.org/10.3390/rs13050968

Levy, R., Zaunbrecher, R., Fontenot, K. A., Deshotel, V., Price, P. P., III, Hebert, J. P., et al. (2025). *2025 rice varieties & management tips*. LSU AgCenter.

Liu, N. (2024). *Crop mapping using deep learning and multi-source satellite remote sensing*. https://doi.org/10.5525/GLA.THESIS.84306

LSU AgCenter. (2025). *Acadia Parish Profile*. LSU AgCenter. https://www.lsuagcenter.com/portals/our_offices/parishes/acadia/features/parish_profile

Lv, Z., Zhang, X., & Benediktsson, J. A. (2017). Developing a general post-classification framework for land-cover mapping improvement using high-spatial-resolution remote sensing imagery. *Remote Sensing Letters*, *8*(7), 607–616. https://doi.org/10.1080/2150704X.2017.1306137

Macedo, I., Pittelkow, C. M., Terra, J. A., Castillo, J., & Roel, A. (2024). The power of on-farm data for improved agronomy. *Global Food Security*, *40*, 100752. https://doi.org/10.1016/j.gfs.2024.100752

Mahendra, H. N., Mallikarjunaswamy, S., Basavaraju, N. M., Poojary, P. M., Gowda, P. S., Mukunda, M., Navya, B., & Pushpalatha, V. (2022). Deep Learning Models For Inventory of Agriculture Crops and Yield Production Using Satellite Images. *2022 IEEE 2nd Mysore Sub Section International Conference (MysuruCon)*, 1–7. https://doi.org/10.1109/MysuruCon55714.2022.9972523

Muñoz-Sabater, J., Dutra, E., Agustí-Panareda, A., Albergel, C., Arduini, G., Balsamo, G., et al. (2021). ERA5-Land: A state-of-the-art global reanalysis dataset for land applications. *Earth System Science Data*, *13*(9), 4349–4383. https://doi.org/10.5194/essd-13-4349-2021

Nikparvar, B., & Thill, J.-C. (2021). Machine Learning of Spatial Data. *ISPRS International Journal of Geo-Information*, *10*(9), 600. https://doi.org/10.3390/ijgi10090600

Nossam, S. C., Katakam, R. A., Pulastya, G., & Venugopalan, M. (2024). Enhanced Crop Yield Prediction using Machine Learning Techniques. *2024 15th International Conference on Computing Communication and Networking Technologies (ICCCNT)*, 1–6. https://doi.org/10.1109/ICCCNT61001.2024.10724901

Rahman, N. S. A., Arifin, K., & Aiyub, K. (2025). Advancing global food security via multidimensional strategies for sustainable paddy productivity. *Multidisciplinary Reviews*, *9*(3), 2026097. https://doi.org/10.31893/multirev.2026097

Ray, D. K., Gerber, J. S., MacDonald, G. K., & West, P. C. (2015). Climate variation explains a third of global crop yield variability. *Nature Communications*, *6*(1), 5989. https://doi.org/10.1038/ncomms6989

Shojaeezadeh, S. A., Elnashar, A., & David Weber, T. K. (2025). A novel fusion of Sentinel-1 and Sentinel-2 with climate data for crop phenology estimation using Machine Learning. *Science of Remote Sensing*, *11*, 100227. https://doi.org/10.1016/j.srs.2025.100227

Soni, Dr. G. (2025). Comprehensive Study and Review of Thirty Key Research Contributions on Artificial Intelligence in the Field of Agricultural. *International Journal for Research in Applied Science and Engineering Technology*, *13*(9), 1065–1074. https://doi.org/10.22214/ijraset.2025.74167

Strobl, C., Boulesteix, A.-L., Zeileis, A., & Hothorn, T. (2007). Bias in random forest variable importance measures: Illustrations, sources, and a solution. *BMC Bioinformatics*, *8*(1), 25. https://doi.org/10.1186/1471-2105-8-25

Tornos, L., Huesca, M., Dominguez, J. A., Moyano, M. C., Cicuendez, V., Recuero, L., & Palacios-Orueta, A. (2015). Assessment of MODIS spectral indices for determining rice paddy agricultural practices and hydroperiod. *ISPRS Journal of Photogrammetry and Remote Sensing*, *101*, 110–124. https://doi.org/10.1016/j.isprsjprs.2014.12.006

USGS. (2025, July 18). *How do I use a scale factor with Landsat Level-2 science products? | U.S. Geological Survey*. https://www.usgs.gov/faqs/how-do-i-use-a-scale-factor-landsat-level-2-science-products (last accessed 11 August 2026)

Van Klompenburg, T., Kassahun, A., & Catal, C. (2020). Crop yield prediction using machine learning: A systematic literature review. *Computers and Electronics in Agriculture*, *177*, 105709. https://doi.org/10.1016/j.compag.2020.105709

Vashisth, A., K. S., A., Raj H, C., Kundu, M., & Krishnan, P. (2026). Crop Yield Prediction Using Remote Sensing and Machine Learning Techniques: A Comprehensive Review. *Frontiers in Remote Sensing*, *7*. https://doi.org/10.3389/frsen.2026.1840405

Verma, V., Vishal, B., Kohli, A., & Kumar, P. P. (2021). Systems-based rice improvement approaches for sustainable food and nutritional security. *Plant Cell Reports*, *40*(11), 2021–2036. https://doi.org/10.1007/s00299-021-02790-6

Wang, L., Chen, Z., Liu, W., & Huang, H. (2024). A Temporal–Geospatial Deep Learning Framework for Crop Yield Prediction. *Electronics*, *13*(21), 4273. https://doi.org/10.3390/electronics13214273

Wooldridge, J., M. (2010). *Econometric analysis of cross section and panel data* (2nd ed.). MIT Press, Cambridge, MA.

Wulder, M. A., Loveland, T. R., Roy, D. P., Crawford, C. J., Masek, J. G., Woodcock, C. E., et al. (2019). Current status of Landsat program, science, and applications. *Remote Sensing of Environment*, *225*, 127–147. https://doi.org/10.1016/j.rse.2019.02.015

Xiao, G., Huang, J., Zhuo, W., Huang, H., Song, J., Du, K., et al. (2025). Progress and Perspectives of Crop Yield Forecasting With Remote Sensing: A review. *IEEE Geoscience and Remote Sensing Magazine*, *13*(3), 338–368. https://doi.org/10.1109/MGRS.2025.3571906

You, J., Li, X., Low, M., Lobell, D., & Ermon, S. (2017). Deep Gaussian Process for Crop Yield Prediction Based on Remote Sensing Data. *Proceedings of the AAAI Conference on Artificial Intelligence*, *31*(1). https://doi.org/10.1609/aaai.v31i1.11172

Yun, S. D., & Gramig, B. M. (2022). Spatial Panel Models of Crop Yield Response to Weather: Econometric Specification Strategies and Prediction Performance. *Journal of Agricultural and Applied Economics*, *54*(1), 53–71. https://doi.org/10.1017/aae.2021.29

Zhang, C., Diao, C., & Guo, T. (2023). GeoAI for Agriculture. In S. Gao, Y. Hu, & W. Li, *Handbook of Geospatial Artificial Intelligence* (1st ed., pp. 330–350). CRC Press, Boca Raton, FL. https://doi.org/10.1201/9781003308423-16

Zhu, Z., Wulder, M. A., Roy, D. P., Woodcock, C. E., Hansen, M. C., Radeloff, V. C., et al. (2019). Benefits of the free and open Landsat data policy. *Remote Sensing of Environment*, *224*, 382–385. https://doi.org/10.1016/j.rse.2019.02.016